基于 Melt-in-Tube 法制备的特种光纤及其应用

张晔明[1]，邱建荣[1,2*]

[1]华南理工大学材料科学与工程学院，广东 广州 510641；

[2]浙江大学光电科学与工程学院，浙江 杭州 310027

摘要 针对化学气相沉积法制备的光纤组分变化范围受限的问题，介绍了近年来发展迅速的光纤拉丝法(MIT)，并从预制棒芯原料为玻璃、半导体、晶体角度总结归纳近年来 MIT 法制备特种光纤的重要进展，分析了所制备特种光纤的性能和应用特点。最后对这种拉制光纤的方法存在的问题和未来发展趋势进行了展望。

关键词 光纤制备；光纤拉丝法(MIT)；特种光纤；光纤应用

中图分类号 TQ171 **文献标识码** A **doi**：10.3788/LOP56.170601

Fabrication and Application of Special Optical Fibers Using Melt-in-Tube Method

Zhang Yeming[1], Qiu Jianrong[1,2*]

[1] *School of Materials Science and Engineering, South China University of Technology, Guangzhou, Guangdong* 510641, *China*;

[2] *College of Optical Science and Engineering, Zhejiang University, Hangzhou, Zhejiang* 310027, *China*

Abstract Considering the problem that the optical fibers prepared via the modified chemical vapor deposition method suffer from the restriction of limited variation range of fiber core components, the rapidly developed melt-in-tube (MIT) fiber drawing method is introduced. The recent progress in the preparation of special optical fibers based on the MIT method is summarized from the perspective of glass core fiber, semiconductor core fiber, and crystal core fiber. Further, the performances and applications of these optical fibers are also analyzed. Finally, the existing problems and development trend of this method are discussed from a practical perspective.

Key words fabrication of optical fiber; melt-in-tube (MIT) method; special optical fiber; optical fiber application

OCIS codes 160.2290; 190.4370; 140.3510

1 引 言

低损耗石英光纤作为一种理想的光波导，可应用于连接世界的光通信管道、医学治疗、激光、环境传感和精密加工等诸多领域[1-2]。自 1960 年至今，商用的石英光纤损耗已趋近于极限理论最小值(0.15 dB/km)，形成了完备的上下游产业。但石英材料传输窗口主要在近红外区域，且其非线性效应不占优势，为解决这个问题，最根本的方式是开发新的光纤材料组分[3]。目前基于改进的化学气相沉积(MCVD)技术制备的玻璃光纤的组分范围十分有限，这是因为掺杂不同的目标离子需要相应的卤化物原料，并且可掺杂浓度通常受到限制[4]。不论是科学研究还是实际应用，都需要研究一种新的、具有普适性的适用于各种功能光纤制备的新方法。

2 光纤拉丝法

除 MCVD 法外，管棒法(rod-in-tube)是应用最多的光纤制备方法。其工艺通常为：分别制备纤芯和包层玻璃，然后加工成纤芯棒和套管制成预制棒，在高温下将纤芯和套管同时软化拉制成光纤。Melt in tube(MIT)法制备光纤具有类似的操作流程，但

收稿日期：2019-04-03；**修回日期**：2019-04-26；**录用日期**：2019-05-09

基金项目：国家重点科研项目(2018YFB1107200)、国家自然科学基金(51772270)

* **E-mail**：qjr@zju.edu.cn

相比于管棒法，包层材料在拉制过程中软化，而纤芯材料呈熔融状态，因此 MIT 法也被称为熔芯法。上述过程对光纤最终的形态影响是多样的，一般认为该过程提供了一个高非平衡态环境，可能导致光纤芯包元素的扩散甚至发生化学反应；同时取决于光纤芯包组分的灵活设计，最终可实现很多特殊的性能。更早期的泰勒线法[5]和软玻璃挥发芯法(VCM)[6]具有一些相似的特点，比如泰勒线最终是在玻璃外壳中制备了很细的金属或合金线，虽然在金属的熔点温度拉制，但是包层玻璃和合金芯没有发生反应。玻璃挥发芯法使用软玻璃和石英管作为预制棒，在拉丝温度时，某些组分，如碱和碱土氧化物挥发掉，纤芯剩余为高硅玻璃。这两种方法由于使用应用范围较局限，不在此文中进行讨论。

图 1 是 MIT 法制备光纤的过程示意图，由高纯粉末/玻璃/陶瓷/晶体和相应包层制成预制棒(此图只显示陶瓷和晶体与石英组成的预制棒)，在特定的拉丝温度下进行拉丝。预制棒在掉棒前纤芯区会有一个熔融过程，纤芯区材料熔融在高温下与包层玻璃发生相互作用，使得该方法有潜力获得具有极端组分的纤芯，甚至是常规方法不能获得的纤芯。有趣的是，在该过程中很多异质芯包材料的热膨胀系数和折射率的匹配问题会自发解决。综上所述，MIT 法具有以下优点：1)极大地拓宽纤芯材料范围；2)避免多组分纤芯材料拉制过程中的异常析晶；3)充分利用纤芯材料和包层玻璃之间的化学反应。除直接拉制外，后续的激光/热处理也被结合起来用以实现更多样的光纤组分。

MIT法制备的光纤可分为三大类：玻璃芯光纤、半导体芯光纤和晶体芯光纤。该分类方法是指光纤预制棒的组成，在拉制后光纤的组分会发生一定的变化，除了半导体芯光纤，其他两种预制棒制备的光纤纤芯最终均呈现玻璃态。

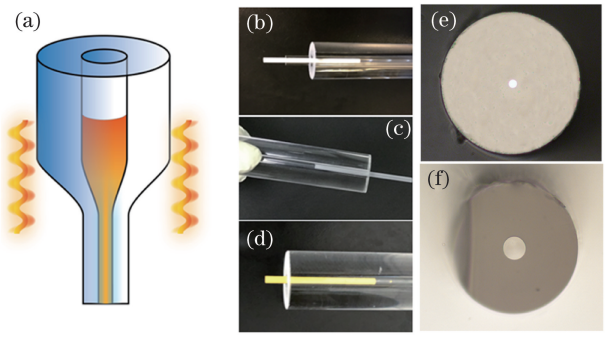

图 1 MIT 法制备光纤。(a)拉制光纤过程示意图；(b)～(d)使用晶体/陶瓷芯的预制棒图；(e)～(f)制备的光纤截面图

Fig. 1 Fabrication of optical fiber by melt-in-tube method. (a) Diagram of fiber drawing process; (b)-(d) fiber preforms based on ceramics or crystals; (e)-(f) cross sections of prepared optical fiber

3 玻璃芯光纤

管棒法是将光纤纤芯玻璃加工为柱状置于包层管中进行拉制，这是一种常用的方法[7]。但是该方法强调光纤的确定性，芯包组分一般为特殊设计的相似成分，其拉制过程只是预制棒的尺度量化缩小，且元素扩散通常认为会破坏光纤性能。相比之下，MIT 法是在熔芯条件下拉制预制棒，目的是为了防止多组分纤芯玻璃的不可控结晶或者是为了获得极端组分。Ballao 等[8]在 1995 年使用高 Tb 含量的 Tb_2O_3-Al_2O_3-SiO_2 粉末作为反应前体，在石英管中进行拉制获得 Tb_2O_3 质量分数超过 50% 的光纤，首次证明了该方法制备包含极端组分的光纤的潜力。另外，因为稀土离子在晶体和玻璃配位场具有不同的发光效率，MIT 法常与后续热处理结合以制备可控析晶的玻璃陶瓷芯光纤。热处理制备微晶玻璃的示意图如图 2 所示，通常使用特殊设计的前驱体玻璃和包层进行拉制得到前驱体光纤，在稍高于纤芯玻璃析晶温度下进行热处理，最终获得具有 nm 尺度晶粒的玻璃陶瓷光纤。由于在小于一定尺寸的纳米晶粒中光的散射损耗较小，因此，这种具有局部均匀晶体场的光纤被认为具有实现单晶性能的潜力[9]。Peng 等[10]用 MIT 法拉制前驱体玻璃光纤，通过热处理制备含有 CaF_2 微晶的玻璃陶瓷光纤，得到更强的上转换发光。Fang 等[11]采用拉制前驱体光纤，通过热处理析出含有 $Ba_2TiSi_2O_8$ 的纳米晶，实现基于光纤的 1030 nm 倍频转换。纳米晶粒的直径可通过后续热处理温度和时间的改变进行调控，从而获得不同光谱性能的光纤。董国平课题组[12-13]采用 MIT 法制备含有可控析晶的 $NaYF_4$ 纳米晶或 PbS 量子点光纤，通过控制不同粒径实现了可调控的发光性能。

另外，Fang 等[14]发现使用 MIT 法在拉制过程中可有效避免某些纤芯成分快速析晶而导致的光纤失透问题，如图 3 所示。

使用玻璃芯(或某种玻璃芯成分的粉体)作为前驱体拉制光纤的工作总结如表 1 所示。可以看到，通过 MIT 方法拉制石英或软玻璃包层光纤可实现不同波段的可调谐宽带发光、激光、高非线性和低本征非线性等不同性能。目前所制备的光纤损耗整体

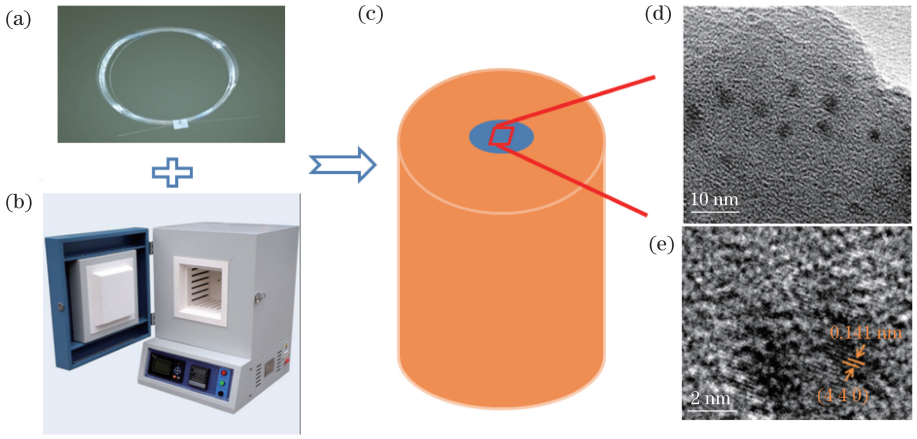

图 2 制备微晶光纤主要工艺。(a)拉制的前驱体光纤;(b)马弗炉处理;(c)微晶光纤;(d)(e)一定尺寸的纳米晶颗粒

Fig. 2 Main processes for fabricating microcrystalline optical fiber. (a) Drawn precursor fiber; (b) muffle furnace process; (c) microcrystalline optical fiber; (d)(e) nanocrystalline particles with certain size

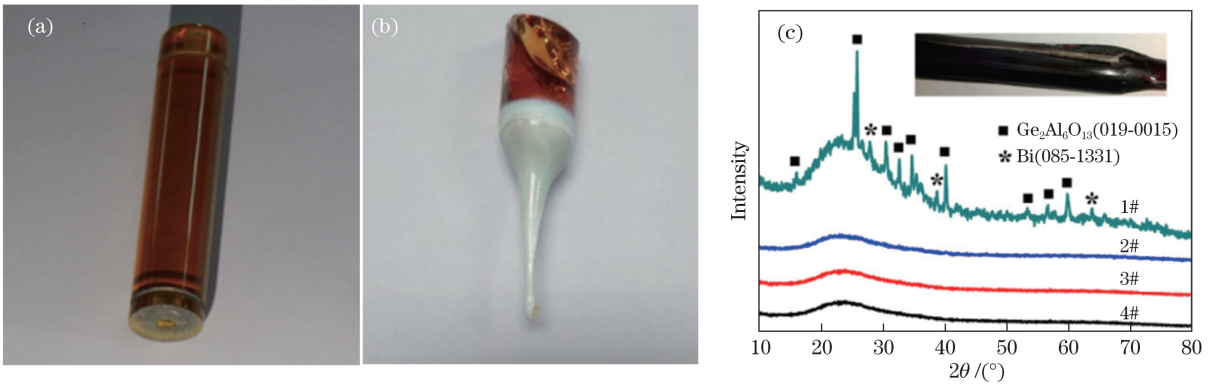

图 3 MIT 法获得微晶光纤的析晶过程。(a)拉制前的玻璃棒;(b)常规拉制过程玻璃棒快速析晶而失透;(c) 1 # ～4 # 试样的 X 射线衍射图(1 # 为拉制后出现不可控析晶的玻璃棒,2 # 为拉制前玻璃棒,3 # 为结晶后二次熔融玻璃,4 # 为 MIT 法拉制的光纤芯,插图为普通拉制后失透的玻璃芯)

Fig. 3 Crystallization process in microcrystalline optical fiber by MIT method. (a) Glass rod before drawing process; (b) crystallization appears in bottom after drawing process and glass rod turns to opaque; (c) X-ray diffraction patterns of samples 1 #-4 # (1 # represents uncontrolled crystallized glass rod after drawing, 2 # represents glass rod before drawing, 3 # represents secondary melted glass after crystallization, 4 # represents optical fiber core drawn by MIT method, and insert is opaque glass after common drawing process)

较高,主要是由纤芯部位的纳米晶散射损耗和加工过程中引入的杂质/缺陷损耗造成的。为了实用化,需要进一步提高原料纯度并优化加工过程。

4 半导体芯光纤

使用 MIT 法制备高结晶度的半导体芯光纤是另一个很活跃的研究方向。半导体光纤具有在 μm 尺度波导中实现光学和电学性能统一的潜力,且具有高非线性和光电性能,适用于信号处理,可成为下一代光电应用设备。Ballato 等[22]在 2008 年制备硅芯光纤,将半导体光纤成分从一元发展到二元甚至多元。2010 年 Ballato 等[23]拉制了 InSb 二元合金,证明可拉制更高晶体复杂度的半导体芯。2015 年 Tang 等[24-25]制备 Se、Te 一元和 SeTe 二元合金。半导体芯光纤研究的进一步发展包括:1)使用激光后处理半导体光纤纤芯提高取向度甚至诱导出单晶芯[26-27]。如图 4 所示,通过激光照射光纤,相当于在包层中二次熔融芯层,在光纤特殊的波导环境下会产生一个高温高压的环境,最终可实现芯区半导体取向和带隙能量的调控。2)使用碱/碱土氧化物隔绝层以降低氧的污染[28]。3)基于原位的化学反应通过廉价芯棒获得高纯度 Si 芯半导体光纤[29]。图 5 所示为使用廉价的 Al 棒和石英管基于原位的化学反应获得高纯度 Si 半导体光纤的实验。

表 1 玻璃芯光纤

Table 1 Optical fiber with glass core

Preform		Drawing temperature /℃	Crystallization temperature /℃	Application / performance	Transmission loss /(dB·m^{-1})	Reference
Core (glass)	Cladding					
$60.9SiO_2$-$16Al_2O_3$-$16ZnO$-$7TiO_2$-$0.1Cr_2O_3$	Silica tube	1830	850	Broadband emission in 600-800 nm	-	[15]
$64SiO_2$-$23Ga_2O_3$-$13Li_2O$-$0.1NiO$	Silica tube	1830	800	Broadband emission in near infrared	-	[16]
$25.5Li_2O$-$21.5Ta_2O_5$-$35.3SiO_2$-$17.6Al_2O_3$-$0.15NiO$	Silica tube	1950	800	Broadband emission in 1140-1620 nm	-	[17]
$60B_2O_3$-$8Bi_2O_3$-$32CaF_2$-$1YbF_3$-$0.5ErF_3$	Commercial BK7 glass tube	1000	530	100 times upconversion luminescence enhancement	-	[10]
$45SiO_2$-$5Al_2O_3$-$35BaO$-$15TiO_2$	Silica tube	1830	850	Second harmonic effect	8.1(@532 nm)	[11]
$37B_2O_3$-$28SiO_2$-$18Na_2O$-$7NaF$-$10YF_3$-$2ErF_3$-x HoF_3 (x=0, 1, 2, 3)	Commercial BK7 glass tube	950	470-500	Mid-infrared emission in 2.6-2.95 μm	11.3(@1310 nm)	[12]
$40B_2O_3$-$25SiO_2$-$18Na_2O$-$7NaF$-$10YF_3$-$2ErF_3$	Commercial BK7 glass tube	950	470-500	Enhanced emission in 2.7 μm	7.4(@1310 nm)	[18]
$66SiO_2$-$8B_2O_3$-$18K_2O$-$6ZnO$-$2ZnS$-$1PbO$	Silica tube	1830	560-600	Broadband luminescence in 1-2 μm	-	[13]
1*: $52B_2O_3$-$15Na_2O$-$15K_2O$-$13ZnO$-$5Al_2O_3$-$1PbO$-$1ZnS$ 2*: $25SiO_2$-$35B_2O_3$-$25Na_2O$-$10ZnO$-$5BaO$-$1PbO$-$1ZnS$	1*: commercial borosilicate glass tube #1 2*: commercial borosilicate glass tube #2	1*: 1000 2*: 950	390-410	Controllable grain size corresponds to tunable 1.0-1.8 μm emission	14.4-27.1 (@1310 nm)	[19]
$50SiO_2$-$30GeO_2$-$15MgO$-$5Al_2O_3$-$1.0Bi_2O_3$	Silica tube	1830	-	Broadband emission in near infrared	6.9(@1310 nm)	[14]
SrO/Al_2O_3 (5∶8 in mol)	Silica tube	1925	-	≈0 brillouin frequency thermal coefficient	2.7(@1534 nm)	[20]
SrF_2/Al_2O_3 powder	Silica tube	2000	-	Low intrinsic nonlinearity	0.7-2.7 (@1534 nm)	[21]

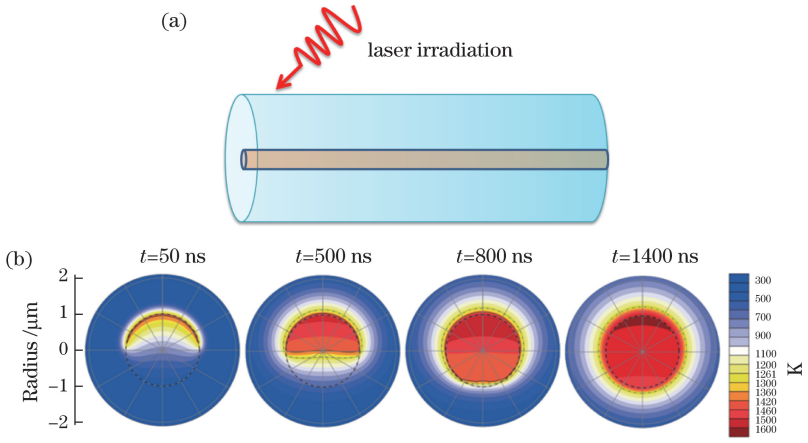

图 4 激光对光纤加工处理。(a)激光后处理光纤示意图;(b)光纤受到激光照射后温度分布

Fig. 4 Laser processing on optical fibers. (a) Diagram of laser post-processing on optical fiber; (b) temperature distributions of fiber after laser irradiation

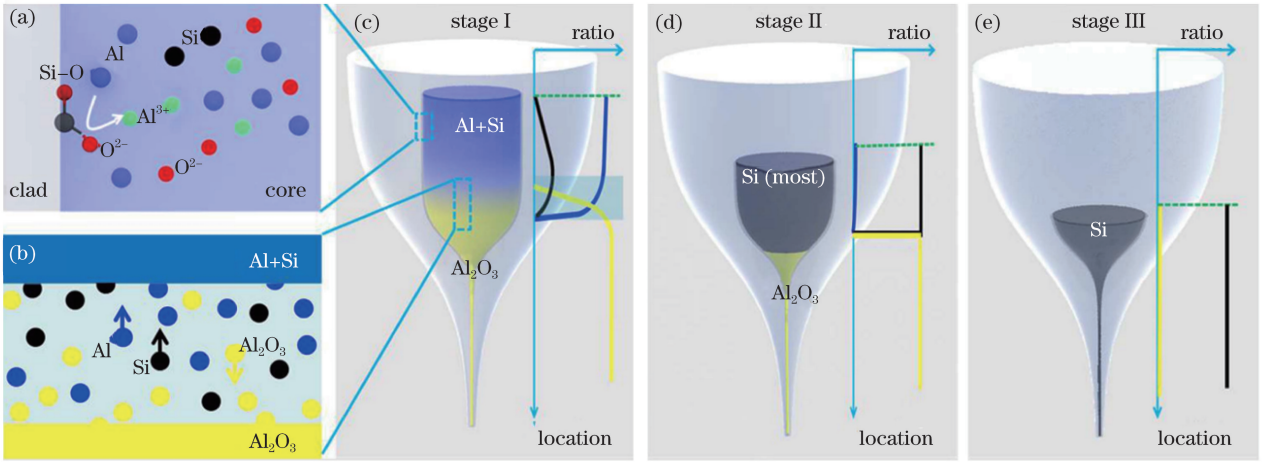

图 5 光纤拉制过程中的原位化学反应。(a)(b) 预制棒拉制过程中化学反应和元素迁移；(c)～(e)预制棒拉制的前中后段纤芯成分的变化

Fig. 5 *In-situ* chemical reaction in fiber drawing process. (a)(b) Chemical reaction and element migration during drawing process; (c)-(e) changes of core composition in different stages of fiber drawing process

半导体光纤的详细文献总结如表 2 所示，随着使用 MIT 法制备半导体光纤的工艺日益成熟，其可应用在传感器、光电探测、红外非线性光子光学、太赫兹波导等领域。为降低半导体芯光纤的损耗，可从减小多晶纤芯的晶界损耗，避免氧对纤芯的污染等方面考虑。在半导体芯光纤高效接入石英基光纤网络这一方向上，已出现利用半导体光纤锥头耦合来减小耦合损耗等新思路[30]，如图 6 所示。

表 2 半导体芯光纤

Table 2 Optical fiber with semiconductor core

Preform		Drawing temperature /℃	Application performance	Transmission loss /(dB·cm^{-1})	Reference
Core	Cladding				
Bi_2Se_3 powder	Commercial K9 glass	840	Thermoelectric performance	-	[31]
Se/Te powder (1∶1 in mol)	Multicomponent phosphate glass	660	Stress sensing/ optical detection	2.6(@1310 nm)	[32]
Sb_2Se_3 powder	Multicomponent phosphate glass	660	Temperature sensor photoelectric detector	-	[33]
Se/Te powder (4∶1 in mol)	Multicomponent phosphate glass	660	Optical switch and photoelectric detector	2.0(@1550 nm)	[24]
Te powder	Multicomponent phosphate glass	660	Far infrared/terahertz waveguide	Too high	[25]
In/Se powder (4∶3 in mol)	Commercial borosilicate glass tube	900	Thermoelectric integrated	-	[34]
Bi_2Te_3 powder	Commercial borosilicate glass tube	900	Thermoelectric optical fiber	-	[35]
SnSe powder	Commercial borosilicate glass tube	900	Thermoelectric integrated	-	[36]
Al rod	Silica tube	2200	Crystalline silicon fiber	-	[29]
GaSb pellet	Duran glass tube AR glass tube	Torch flame/laser processing	Near infrared photoluminescence/ adjustable band gap	-	[37]
Silicon rod/CaO coating	Silica tube	Oxyacetylene flame	Nonlinear photonics applications in infrared	1-2.5(1500-2500 nm)	[38]
Silicon rod/ oxide coating	Silica tube	Oxyacetylene flame		3.8-20(@1550 nm)	[28]

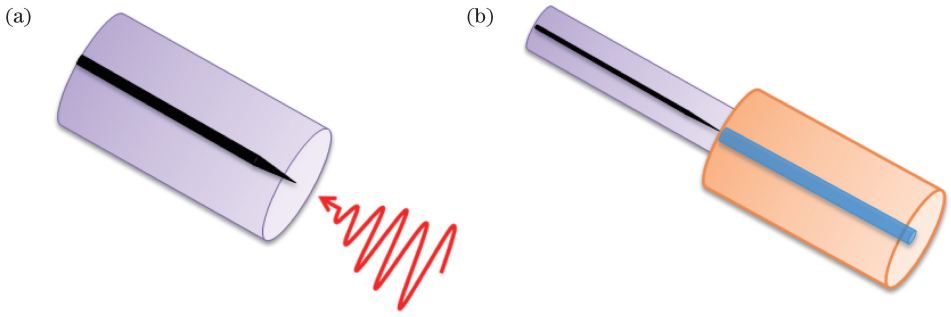

图 6 半导体光纤接入石英光纤网络。(a)半导体芯光纤锥头的空间光耦合;(b)单模光纤与半导体芯光纤锥头耦合

Fig. 6 Semiconductor fiber connected with silica optical fiber network. (a) Coupling of spatial optical light and tapered semiconductor core optical fiber; (b) coupling of tapered semiconductor core optical fiber and single-mode fiber

5 晶体芯光纤

晶体作为预制棒芯拉制光纤最初源于 Cr∶YAG 的尝试。在 2006 年,Huang 等[39]试图通过 Cr∶YAG 和石英包层拉制一定结晶度的晶体芯的双包层光纤,虽然该尝试最终被证明是无效的,且所有后续实验都表明这种组合会得到一种钇铝硅酸盐(YAS)全玻璃的纤芯,但这种大胆的尝试打开一个新的领域,即通过 MIT 法,将各种性能的晶体和石英包层相结合,在充分考虑纤芯材料和包层玻璃相互作用的情况下,可以获得具有新性能的光纤。YAG 晶体具有高稳定性和优异的光学性能,是目前使用最为广泛的晶体。由于 Y 离子可实现和稀土离子的任意比掺杂,YAG 常常作为一种优异的稀土离子引入前体运用到 MIT 法中制备光纤。目前,由不同浓度的 Cr、Nd、Er、Yb、Tm 掺杂的 YAG 单晶、多晶陶瓷已被作为预制棒以尝试拉制。所制备的 RE∶YAS 光纤可应用于激光、单频激光等领域[40]。图 7 是基于稀土掺杂的 YAS 光纤激光器的应用,这种 YAS 光纤具有较高的 Al、Y 含量,使得其相对于石英基光纤玻璃网络结构更复杂,可实现非常灵活的稀土离子掺杂制度(掺杂种类、掺杂浓度),同时本征非线性极大

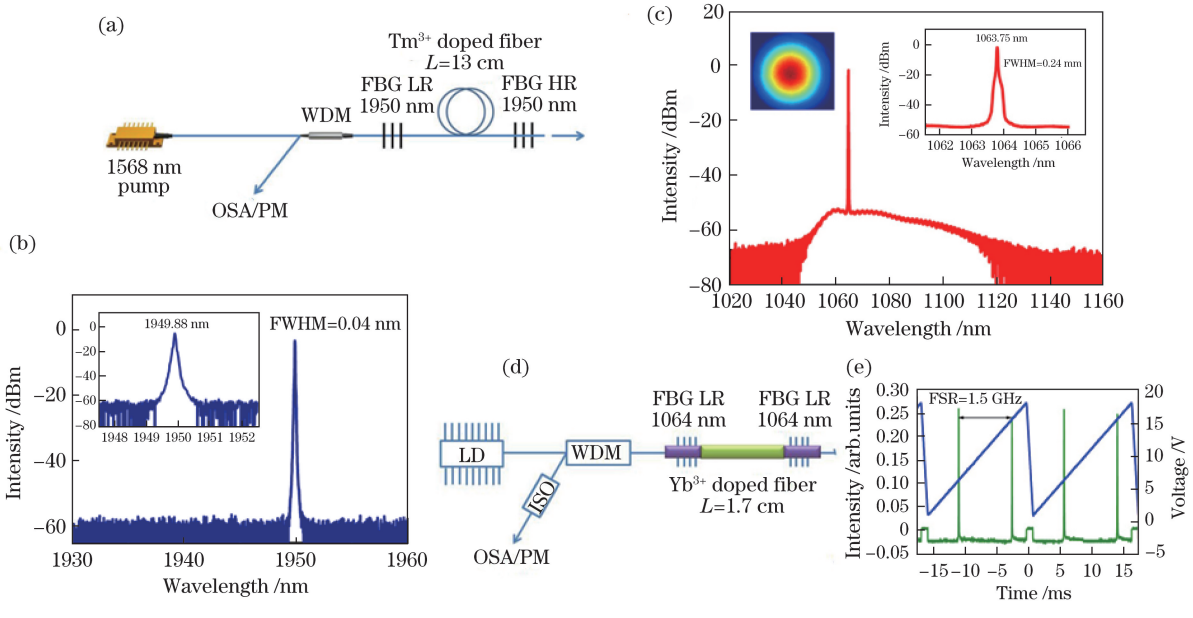

图 7 YAS 光纤在激光方面的应用。(a)基于 Tm∶YAS 光纤的全光纤线性腔示意图;(b) Tm∶YAS 实现的2.0 μm 激光出射;(c) Nd∶YAS 实现的1.0 μm 激光(插图是所搭建的全光纤激光器的近场能量分布);(d) 基于高掺杂 Yb∶YAS 的分布式布拉格反射(DBR)激光器示意图;(e)实现的单频激光纵模特性

Fig. 7 Laser applications of YAS fiber. (a) Diagram of all-fiber linear cavity based on Tm∶YAS fiber; (b) 2.0 μm laser output spectrum of Tm∶YAS fiber laser; (c) 1.0 μm laser output spectrum of Nd∶YAS fiber laser (insert is near-field energy distribution of home made all-fiber laser); (d) diagram of DBR fiber laser with highly doped Yb∶YAS; (e) longitudinal mode characteristics of single frequency fiber laser

降低，在激光应用方面很有潜力。

其他晶体如 Al_2O_3、LuAG、尖晶石($MgAl_2O_4$)也被尝试用来制备光纤[41-43]，具体参见表 3。将上述晶体作为前驱体制备的光纤，一般最终获得的是一种多组分玻璃。2012 年 Ballao 等[44]出于对非线性的考虑，发现 Al_2O_3 晶体作为预制棒芯获得的光纤芯区可实现极高含量的 Al，因此光纤的非线性仅为商用石英光纤的 1/100，可应用于高能激光。以晶体前驱体作为纤芯并结合 MIT 法获得的玻璃光纤具有较低的损耗，便于与石英光纤系统熔接，与石英光纤相比具有较低的本征非线性，在高能激光领域占有优势。

表 3 晶体芯光纤

Table 3 Optical fiber with crystal core

Preform		Drawing temperature /℃	Application performance	Transmission loss /(dB·m^{-1})	Reference
Core (rod)	Cladding				
Cr:YAG	Silica tube	2025	Near infrared broadband amplification in 1.2-1.6 μm	20(@1550 nm)	[39]
Er:YAG	Silica tube	2025	Emission similar to erbium doped fiber amplifier (EDFA) higher doping concentration	0.15-0.2 (@1300 nm)	[44]
Yb:YAG	Silica tube	2000	Reduced stimulated Brillouin	0.1(@1.3 μm)	[45]
Yb:YAG	Silica tube	2000 (post feeding)	≈4 W laser output	2.2(@1200 nm)	[46]
Nd:YAG	Silica tube			1.5(@1200 nm)	[47]
Nd:YAG	Silica tube	2000	Low threshold all-fiber laser	8.2(@1550 nm)	[48]
Tm:YAG	Silica tube	2000	Fiber laser in 2 μm	9.2(@1550 nm)	[49]
Yb:YAG	Silica tube	2000	Single-frequency laser output	5.6(@1550 nm)	[40]
Yb:YAG/Al_2O_3	Silica tube	2000	High nonlinearity low Brillouin gain	0.7(@1550 nm)	[50]
Al_2O_3	Silica tube	2100	Ultra-low Brillouin gain	0.2(@1534 nm)	[41]
LuAG	Silica tube	2025	Sensitive stress sensing	1.5(@1534 nm)	[42]
$MgAl_2O_4$	Silica tube	2175	Highly acoustically-anti-guiding waveguide properties	0.2(@1534 nm)	[43]

6 结 论

通过 MIT 法制备光纤可根据预制棒芯的不同归为 3 大类：玻璃前驱体芯、半导体前驱体芯、晶体前驱体芯。这些光纤在拉制过程中均会经历一个纤芯熔融过程，在拉丝环境提供的高非平衡态下可能出现芯包元素的迁移及芯包间的化学反应，最终获得常规方法不能获得的纤芯组分。通过设计芯包组分，可实现很多具有特殊性能的光纤，在高能激光应用、光纤传感、可调谐宽带发光、高/低非线性、太赫兹波导、新一代光电设备等领域具有一定的应用潜力。目前存在的挑战主要是降低光纤损耗及与以石英基光纤为主的光网络系统的互联问题。未来的研究方向是在解决现有问题的基础上，进一步扩展纤芯材料的范围，对芯包组分进行大胆创新并获得具有特殊性能的光纤，并将其积极地应用于实践。

参 考 文 献

[1] Liao Y B, Yuan L B, Tian Q. The 40 years of optical fiber sensors in China[J]. Acta Optica Sinica, 2018, 38(3): 0328001.
廖延彪, 苑立波, 田芊. 中国光纤传感 40 年[J]. 光学学报, 2018, 38(3): 0328001.

[2] Liu Y Z, Xing Y B, Xu Z W, *et al*. Research progress in high power Tm^{3+}-doped silica fiber lasers[J]. Laser & Optoelectronics Progress, 2018, 55(5): 050004.
刘茵紫, 邢颖滨, 徐中巍, 等. 高功率掺铥石英光纤激光器研究进展[J]. 激光与光电子学进展, 2018, 55(5): 050004.

[3] Liu Z J, Bian J Y, Huang Y, *et al*. Research progress on rare earth ions doped chalcogenide fiber for mid-infrared luminescence[J]. Laser & Optoelectronics Progress, 2017, 54(2): 020003.
刘自军, 卞俊轶, 黄炎, 等. 稀土掺杂硫系光纤中红外发光的研究进展[J]. 激光与光电子学进展, 2017,

54(2): 020003.

[4] Wang Y B, Li J Y. Status and development tendency of high power ytterbium doped fibers[J]. Chinese Journal of Lasers, 2017, 44(2): 0201009.
王一磷, 李进延. 高功率掺镱光纤的现状及发展趋势[J]. 中国激光, 2017, 44(2): 0201009.

[5] Taylor G F. A method of drawing metallic filaments and a discussion of their properties and uses[J]. Physical Review, 1924, 23(5): 655-660.

[6] Snitzer E, Tumminelli R. SiO_2-clad fibers with selectively volatilized soft-glass cores[J]. Optics Letters, 1989, 14(14): 757-759.

[7] Wang W C, Zhou B, Xu S H, *et al*. Recent advances in soft optical glass fiber and fiber lasers[J]. Progress in Materials Science, 2019, 101: 90-171.

[8] Ballato J, Snitzer E. Fabrication of fibers with high rare-earth concentrations for Faraday isolator applications[J]. Applied Optics, 1995, 34(30): 6848-6854.

[9] Tick P A, Borrelli N F, Reaney I M. The relationship between structure and transparency in glass-ceramic materials[J]. Optical Materials, 2000, 15(1): 81-91.

[10] Peng W C, Fang Z J, Ma Z J, *et al*. Enhanced upconversion emission in crystallization-controllable glass-ceramic fiber containing Yb^{3+}-Er^{3+} codoped CaF_2 nanocrystals[J]. Nanotechnology, 2016, 27(40): 405203.

[11] Fang Z J, Xiao X S, Wang X, *et al*. Glass-ceramic optical fiber containing $Ba_2TiSi_2O_8$ nanocrystals for frequency conversion of lasers[J]. Scientific Reports, 2017, 7: 44456.

[12] Kang S L, Yu H, Ouyang T C, *et al*. Novel Er^{3+}/Ho^{3+}-codoped glass-ceramic fibers for broadband tunable mid-infrared fiber lasers[J]. Journal of the American Ceramic Society, 2018, 101(9): 3956-3967.

[13] Huang X J, Fang Z J, Peng Z X, *et al*. Formation, element-migration and broadband luminescence in quantum dot-doped glass fibers[J]. Optics Express, 2017, 25(17): 19691-19700.

[14] Fang Z J, Zheng S P, Peng W C, *et al*. Bismuth-doped multicomponent optical fiber fabricated by melt-in-tube method[J]. Journal of the American Ceramic Society, 2016, 99(3): 856-859.

[15] Fang Z J, Zheng S P, Peng W C, *et al*. Fabrication and characterization of glass-ceramic fiber-containing Cr^{3+} doped $ZnAl_2O_4$ nanocrystals[J]. Journal of the American Ceramic Society, 2015, 98(9): 2772-2775.

[16] Fang Z J, Zheng S P, Peng W C, *et al*. Ni^{2+} doped glass ceramic fiber fabricated by melt-in-tube method and successive heat treatment[J]. Optics Express, 2015, 23(22): 28258-28263.

[17] Yu Y Z, Fang Z J, Ma C S, *et al*. Mesoscale engineering of photonic glass for tunable luminescence[J]. NPG Asia Materials, 2016, 8(10): e318.

[18] Kang S L, Fang Z J, Huang X J, *et al*. Precisely controllable fabrication of Er^{3+}-doped glass ceramic fibers: novel mid-infrared fiber laser materials[J]. Journal of Materials Chemistry C, 2017, 5(18): 4549-4556.

[19] Huang X J, Fang Z J, Kang S L, *et al*. Controllable fabrication of novel all solid-state PbS quantum dot-doped glass fibers with tunable broadband near-infrared emission[J]. Journal of Materials Chemistry C, 2017, 5(31): 7927-7934.

[20] Cavillon M, Furtick J, Kucera C J, *et al*. Brillouin properties of a novel strontium aluminosilicate glass optical fiber[J]. Journal of Lightwave Technology, 2016, 34(6): 1435-1441.

[21] Cavillon M, Kucera C J, Hawkins T W, *et al*. Oxyfluoride core silica-based optical fiber with intrinsically low nonlinearities for high energy laser applications[J]. Journal of Lightwave Technology, 2018, 36(2): 284-291.

[22] Ballato J, Hawkins T, Foy P, *et al*. Silicon optical fiber[J]. Optics Express, 2008, 16(23): 18675-18683.

[23] Ballato J, Hawkins T, Foy P, *et al*. Binary III-V semiconductor core optical fiber[J]. Optics Express, 2010, 18(5): 4972-4979.

[24] Tang G W, Qian Q, Wen X, *et al*. Reactive molten core fabrication of glass-clad $Se_{0.8}Te_{0.2}$ semiconductor core optical fibers[J]. Optics Express, 2015, 23(18): 23624-23633.

[25] Tang G W, Qian Q, Wen X, *et al*. Phosphate glass-clad tellurium semiconductor core optical fibers[J]. Journal of Alloys and Compounds, 2015, 633: 1-4.

[26] Healy N, Mailis S, Bulgakova N M, *et al*. Extreme electronic bandgap modification in laser-crystallized silicon optical fibres[J]. Nature Materials, 2014, 13(12): 1122-1127.

[27] Healy N, Fokine M, Franz Y, *et al*. CO_2 laser-induced directional recrystallization to produce single crystal silicon-core optical fibers with low loss[J]. Advanced Optical Materials, 2016, 4(7): 1004-1008.

[28] Nordstrand E F, Dibbs A N, Eraker A J, *et al*. Alkaline oxide interface modifiers for silicon fiber

production[J]. Optical Materials Express, 2013, 3(5): 651-657.

[29] Hou C, Jia X T, Wei L, *et al*. Crystalline silicon core fibres from aluminium core preforms[J]. Nature Communications, 2015, 6: 6248.

[30] McMillen C, Brambilla G, Morris S, *et al*. On crystallographic orientation in crystal core optical fibers II: effects of tapering[J]. Optical Materials, 2012, 35(2): 93-96.

[31] Qian G Q, Sun M, Tang G W, *et al*. High-performance and high-stability bismuth selenide core thermoelectric fibers[J]. Materials Letters, 2018, 233: 63-66.

[32] Huang K M, Tang G W, Luo Q H, *et al*. SeTe alloy semiconductor core optical fibers[J]. Materials Research Bulletin, 2018, 100: 382-385.

[33] Tang G W, Liu W W, Qian Q, *et al*. Antimony selenide core fibers[J]. Journal of Alloys and Compounds, 2017, 694: 497-501.

[34] Sun M, Tang G W, Qian G Q, *et al*. In_4Se_3 alloy core thermoelectric fibers[J]. Materials Letters, 2018, 217: 13-15.

[35] Sun M, Qian Q, Tang G W, *et al*. Enhanced thermoelectric properties of polycrystalline Bi_2Te_3 core fibers with preferentially oriented nanosheets[J]. APL Materials, 2018, 6(3): 036103.

[36] Sun M, Tang G W, Liu W W, *et al*. Sn-Se alloy core fibers[J]. Journal of Alloys and Compounds, 2017, 725: 242-247.

[37] Song S, Healy N, Svendsen S K, *et al*. Crystalline GaSb-core optical fibers with room-temperature photoluminescence[J]. Optical Materials Express, 2018, 8(6): 1435-1440.

[38] Ren H, Shen L, Wu D, *et al*. Nonlinear optical properties of polycrystalline silicon core fibers from telecom wavelengths into the mid-infrared spectral region[J]. Optical Materials Express, 2019, 9(3): 1271-1279.

[39] Huang Y C, Lu Y K, Chen J C, *et al*. Broadband emission from Cr-doped fibers fabricated by drawing tower[J]. Optics Express, 2006, 14(19): 8492-8497.

[40] Zhang Y M, Wang W W, Li J, *et al*. Multi-component yttrium aluminosilicate (YAS) fiber prepared by melt-in-tube method for stable single-frequency laser[J]. Journal of the American Ceramic Society, 2019, 102(2): 2551-2557.

[41] Dragic P, Hawkins T, Foy P, *et al*. Sapphire-derived all-glass optical fibres[J]. Nature Photonics, 2012, 6(9): 627-633.

[42] Dragic D, Pamato G, Iordache V, *et al*. Athermal distributed Brillouin sensors utilizing all-glass optical fibers fabricated from rare earth garnets: LuAG[J]. New Journal of Physics, 2015, 18(1): 015004.

[43] Mangognia A, Kucera C, Guerrier J, *et al*. Spinel-derived single mode optical fiber[J]. Optical Materials Express, 2013, 3(4): 511-518.

[44] Ballato J, Hawkins T, Foy P, *et al*. On the fabrication of all-glass optical fibers from crystals[J]. Journal of Applied Physics, 2009, 105(5): 053110.

[45] Dragic P D, Ballato J, Hawkins T, *et al*. Feasibility study of Yb∶YAG-derived silicate fibers with large Yb content as gain media[J]. Optical Materials, 2012, 34(8): 1294-1298.

[46] Zheng S P, Li J, Yu C L, *et al*. Preparation and characterizations of Yb∶YAG-derived silica fibers drawn by on-line feeding molten core approach[J]. Ceramics International, 2017, 43(7): 5837-5841.

[47] Zheng S P, Li J, Yu C L, *et al*. Preparation and characterizations of Nd∶YAG ceramic derived silica fibers drawn by post-feeding molten core approach[J]. Optics Express, 2016, 24(21): 24248-24254.

[48] Zhang Y M, Qian G Q, Xiao X S, *et al*. A yttrium aluminosilicate glass fiber with graded refractive index fabricated by melt-in-tube method[J]. Journal of the American Ceramic Society, 2018, 101(4): 1616-1622.

[49] Zhang Y M, Qian G Q, Xiao X S, *et al*. The preparation of yttrium aluminosilicate (YAS) glass fiber with heavy doping of Tm^{3+} from polycrystalline YAG ceramics[J]. Journal of the American Ceramic Society, 2018, 101(10): 4627-4633.

[50] Tuggle M, Kucera C, Hawkins T, *et al*. Highly nonlinear yttrium-aluminosilicate optical fiber with a high intrinsic stimulated Brillouin scattering threshold [J]. Optics Letters, 2017, 42(23): 4849-4852.